Applied Radiation and Isotopes 230 (2026) 112483

Contents lists available at ScienceDirect

Applied Radiation and Isotopes

journal homepage: www.elsevier.com/locate/apradiso

Influence of D_2O substitution on BNCT dosimetry with the AB-BNCT system: A combined Monte Carlo and experimental study

Junli Ge [a], Diyun Shu [b,*], Changran Geng [a,c,**], Jinkai Yang [a], Xiaobin Tang [a,c], Yuan-Hao Liu [a,b]

[a] Department of Nuclear Science and Technology, Nanjing University of Aeronautics and Astronautics, Nanjing, Jiangsu Province, 210016, People's Republic of China
[b] Neuboron Therapy System Ltd., Xiamen, Fujian Province, 361000, People's Republic of China
[c] Key Laboratory of Advanced Nuclear Technology and Radiation Protection, Ministry of Industry and Information Technology, Nanjing, Jiangsu Province, 210016, People's Republic of China

ARTICLE INFO

Keywords:
BNCT
D_2O substitution
NeuPex system
Dosimetric performance

ABSTRACT

Boron neutron capture therapy (BNCT) faces challenges in delivering sufficient therapeutic dose to deep-seated tumors due to limited neutron penetration. Previous studies indicate that replacing tissue light water (H_2O) with heavy water (D_2O) can enhance neutron penetration while reducing photon dose under specific conditions. However, the applicability of this method within the NeuPex accelerator-based BNCT system requires further investigation and validation. In this study, Monte Carlo simulations with a radiation computational phantom quantified D_2O substitution effects on BNCT dosimetry for the NeuPex system, complemented by experimental measurements in a water phantom to assess neutron penetration depth and photon dose reduction. Simulation results indicate that when tumor depth exceeds 6 cm, D_2O substitution enhances the dosimetric performance of BNCT within the tumor. At a tumor depth of 7 cm, 20% D_2O substitution increases the tumor minimum dose by 14.1% and D_{80} by 8.2%. Experimental results further demonstrate that D_2O substitution enhances neutron penetration while reducing photon dose contamination. With 20% D_2O substitution, the reaction rate increases beyond depths of approximately 6 cm. This study demonstrates the feasibility and applicability of D_2O substitution in the NeuPex system, establishing a theoretical foundation for future clinical implementation strategies.

1. Introduction

Boron neutron capture therapy (BNCT) has emerged as a promising binary radiotherapy technique requiring targeted boron agent combined with neutron beam (Jin et al., 2022). This modality leverages the nuclear reaction $^{10}B(n,\alpha)^7Li$ within cancer cells to generate high-LET α-particles and ^7Li nuclei. These particles deposit energy over an extremely short range (<10 μm), enabling precise tumor cell destruction while sparing adjacent healthy tissue. BNCT thus offers unique advantages: high selectivity, favorable safety, and short treatment cycles (Barth et al., 2012). In recent years, BNCT has advanced rapidly with the emergence of accelerator-based neutron sources (Kumada et al., 2023). Notably, in 2020, Japan granted regulatory approval to the world's first accelerator-based BNCT (AB-BNCT) system and its companion boron drug for clinical use. Subsequent clinical studies confirmed their efficacy and safety in treating head and neck cancers (Matsumura et al., 2023).

A major clinical challenge for BNCT arises in treating deep-seated tumors, where neutron attenuation within patient tissues leads to insufficient dose at deep depth (Wang et al., 2018). This is primarily due to hydrogen-rich human tissues causing neutron beam degradation through both elastic and inelastic scattering interactions (MacFarlane, 2010). Consequently, patients with deep-seated tumors may be excluded from BNCT clinical studies based on treatment plan evaluation, thereby limiting its applicability for select cases. To enhance the treatment depth of BNCT, heavy water (D_2O) substitution in biological tissues has been proposed (Laissue et al., 1983; Wallace et al., 1995a, 1995b; Green et al., 2021). Since the interaction cross-section between neutrons and deuterium is far lower than that with hydrogen, this substitution can reduce neutron attenuation within the human body. Simultaneously, deuterium substitution reduces photon dose in normal tissues by minimizing neutron capture reactions with hydrogen. It is important to note that D_2O passively diffuses across cell membranes and dynamically

* Corresponding author.
** Corresponding author. Department of Nuclear Science and Technology, Nanjing University of Aeronautics and Astronautics, Nanjing, Jiangsu Province, 210016, People's Republic of China.
E-mail addresses: shudiyun@neuboron.com (D. Shu), gengchr@nuaa.edu.cn (C. Geng).

https://doi.org/10.1016/j.apradiso.2026.112483
Received 2 December 2025; Received in revised form 29 January 2026; Accepted 6 February 2026
Available online 6 February 2026

exchanges with intracellular light water (Berry et al., 2015), suggesting that partial substitution of light water with D_2O in biological tissues is feasible. From a biological perspective, studies confirm that replacing <20% of water with D_2O induces no detectable physiological effects (Shi et al., 2018), whereas concentrations exceeding this threshold may cause mild toxicity in murine models (Kushner et al., 1999). Thus, controlled D_2O substitution of biological water remains theoretically achievable with acceptable toxicological thresholds.

Monte Carlo computational studies have explored the dosimetric benefits of D_2O substitution in BNCT. Wallace et al. (1995a) investigated the impact of D_2O substitution on advantage depth (AD) and treatment depth (TD) using a Snyder head phantom under ideal neutron beam conditions and varying tumor-to-blood boron concentration ratios. Further analysis utilizing the epithermal neutron beam from the JRC/ECN Petten High Flux Reactor (HFR) examined thermal neutron flux and photon depth–dose profiles during both unilateral and bilateral irradiation (Wallace et al., 1995b). Their results demonstrated that D_2O substitution significantly increased both AD and TD. Furthermore, bilateral irradiation with 20% D_2O substitution markedly improved thermal neutron flux uniformity and substantially reduced secondary photon doses. More recently, a University of Birmingham (UK) research team evaluated deuteration's potential using an accelerator-based BNCT system to enhance treatment efficacy for diffuse intrinsic pontine glioma (DIPG) (Green et al., 2021). Their simulations showed that 20% D_2O substitution increased the therapeutic ratio (TR) from 2.0 to 3.0 and raised the minimum tumor dose from 15.5 Gy-Eq to 23 Gy-Eq. Results from both research groups underscore the clinical benefit of integrating deuteration into BNCT.

The Xiamen Humanity Hospital BNCT Center has installed the NeuPex AB-BNCT system independently developed by Neuboron Medical Group. It is currently conducting clinical trials for head and neck tumors as well as clinical research on brain tumors (Zhang et al., 2023). To ensure the applicability of BNCT for treating deep-seated tumors, extensive efforts have been made in neutron beam design and multidirectional irradiation techniques. Beyond conventional approaches, it is hoped that novel methods may further enhance the tumor treatment depth. The substitution of light water in patient tissues with D_2O represents a potential and feasible approach. However, the applicability and scope of this method within the NeuPex system require further investigation and validation. In this study, Monte Carlo simulations using a radiation computational phantom evaluated the impact of D_2O substitution on BNCT dosimetry within the NeuPex system. Concurrently, experimental measurements utilizing a water phantom exposed to the NeuPex neutron beam were performed to examine how D_2O substitution affects neutron penetration and photon dose.

2. Materials and methods

2.1. Tumor-containing radiation computational phantom

A radiation computational phantom, named the Chinese hybrid radiation phantoms (CHRAP), was utilized. CHRAP was independently developed by researchers at Nanjing University of Aeronautics and Astronautics to incorporate distinct Chinese physiological characteristics (Geng et al., 2014). The original anatomical structures were derived from Anatonium™ 3D P1 V5.0, which includes comprehensive modeling of organs, skeleton, blood vessels, and lymph systems (Geng et al., 2014). For this brain tumor-focused investigation, the adult male version of CHRAP was utilized, with retention limited to the head and neck region. A spherical brain tumor model (2.4 cm diameter) was constructed in the right parietal lobe at depths of 5 cm, 6 cm, 7 cm, and 8 cm from the inner skull surface to enable quantitative assessment of depth-dependent effects. Prior to radiation dose calculations, conversion of the phantom geometry into a voxelized format was performed. Tissue structures were defined using Rhinoceros8 software (Lee and Song, 2021) and exported in.obj format. Subsequent voxelization was executed using the 3D Mesh Voxelizer software suite to generate a PHITS-compatible binary text format. A uniform voxel size of 0.17 cm^3 was implemented to achieve an optimal balance between computational accuracy and efficiency. The resulting voxelized phantom data was subsequently imported into PHITS for radiation dose calculations.

2.2. Irradiation planning and dose calculation

To evaluate the effect of D_2O substitution on the BNCT dosimetric performance of the NeuPex system, the voxelized CHRAP was imported into the PHITS Monte Carlo toolkit (version 3.28) (Furuta and Sato, 2021). Tissue density and elemental composition were assigned according to ICRP Publication 89 data (Valentin, 2002). ^{10}B concentration were specified as 25 ppm for normal tissues and 87.5 ppm for the tumor. Based on literature indicating no adverse physiological effects in animals following partial tissue deuteration, D_2O concentrations of 0%, 10%, and 20% were simulated within the phantom. This substitution was implemented through molar replacement of elemental hydrogen in tissue materials with deuterium, where the specified D_2O concentration corresponded directly to the percentage of the material's total hydrogen replaced (Wallace et al., 1995a).

Dose calculations were performed in PHITS using the neutron beam source from the NeuPex system. The neutron beam was modeled with a radius of 19.5 cm, and only a single irradiation field was considered in this study. The complete simulation model is illustrated in Fig. 1, where the yellow line represents the plane passing through the tumor center along the central axis of the radiation beam. The source was positioned laterally within the brain, parallel to the longitudinal body axis, and located 3.5 cm from the skin surface, with its central axis traversing the tumor center. Boron dose rate, fast neutron dose rate, thermal neutron dose rate, and photon dose rate for each voxel were evaluated through the PHITS simulation. To ensure statistical uncertainties below 3%, 5×10^{10} simulated particle histories were used.

2.3. Evaluation of dosimetric parameters in BNCT

Each physical dose rate is multiplied by the corresponding relative biological effectiveness (RBE) or compound biological effectiveness (CBE), yielding the photon-equivalent dose rate. The detailed calculation formula is presented as follows:

$$D_{eq} = D_B \times CBE + D_N \times RBE_N + D_p \times RBE_p$$

where D_{eq} represents the photon-equivalent dose rate. D_B is the boron dose rate. D_N is the neutron dose rate. D_p is the photon dose rate. CBE denotes the compound biological effectiveness for the boron dose, while RBE_N and RBE_p are the relative biological effectiveness for fast neutron dose, thermal neutron dose and photon dose, respectively. Table 1 presents the RBE and CBE values for different dose components across

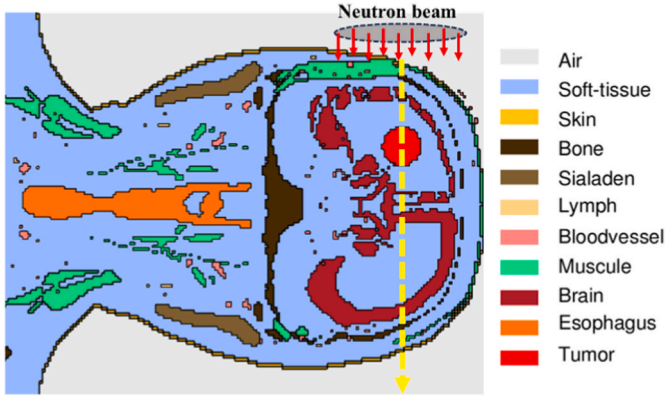

Fig. 1. Monte Carlo simulation model with CHRAP.

Table 1
Biological effectiveness factors for normal tissues and tumor.

Tissue	RBE		CBE
	Photon	Neutron	
Other tissue	1	3.2	1.3
Skin	1	3.2	2.5
Tumor	1	3.2	3.8

various tissues and tumor (Kiger et al., 2008; Coderre and Morris, 1999).

The treatment endpoint is defined by the first instance of any normal tissue reaching its specified dose limit (5 Gy-Eq for the eyes (Takeno et al., 2024); 12 Gy-Eq for the brain (Miyatake et al., 2014) and skin (Igaki, 2022)). The required treatment time is calculated by dividing this limiting dose by its corresponding maximum dose rate. Using this derived treatment time, the photon-equivalent dose distribution is determined throughout the normal tissues and the tumor. These distributions are then presented as Dose-Volume Histograms (DVHs). The DVHs enable calculation of key dose metrics, including maximum dose (D_{max}), minimum dose (D_{min}), mean dose (D_{mean}), D_{80} (dose to 80% of the tumor volume), and the tumor dose homogeneity index, etc.

2.4. Experimental setup for D_2O substitution effect on BNCT neutron beam

In addition to Monte Carlo simulation, experimental measurements were performed to verify the impact of D_2O substitution under the BNCT epithermal neutron beam. All irradiations were conducted at the BNCT Center of Xiamen Humanity Hospital using the NeuPex AB-BNCT system equipped with a 6-cm-radius collimator. The NeuPex system employs proton bombardment of a lithium target to generate neutrons, which are then moderated, shaped, and focused through a beam-shaping assembly to yield an epithermal neutron beam. Operating at a proton energy of 2.35 MeV and a current of 10 mA, the NeuPex beam port delivers an epithermal neutron flux exceeding 1.0×10^9 cm^{-2} s^{-1}.

A water phantom was irradiated by the NeuPex neutron beam (Fig. 2). The phantom exhibited overall external dimensions of 15 cm × 15 cm × 18 cm and featured 1.0-cm-thick PMMA walls, except for the beam-incident face, which had a thickness of 0.5 cm. The phantom was filled with water, 10% D_2O, and 20% D_2O respectively, each to a height of 15 cm from the bottom surface. D_2O solutions were prepared by volumetrically diluting 99.9% pure D_2O with distilled water. The 10% D_2O solution used a 1:9 D_2O-to-distilled water ratio, while the 20% D_2O solution employed a 1:4 ratio (Laissue et al., 1983). During the experimental procedure, the beam central axis was aligned with that of the phantom using the laser system. The incident surface of the phantom was positioned in contact with the beam exit surface at a source-to-surface distance (SSD) of zero.

The depth distribution of the reaction rate within the phantom was measured using neutron activation analysis, with copper selected as the activation detector. Copper strips were positioned along the beam central axis inside the phantom, with dimensions of 15 cm (Fig. 2(a)). Each irradiation cycle for reaction rate measurement lasted 40 min. Following irradiation, the copper strips were sectioned into 1 cm segments. Activated radionuclides were quantified using a high-purity germanium (HPGe) detector, allowing derivation of reaction rates. The reaction rate depth distribution provides a partial reflection of the neutron intensity distribution within the phantom. Photon dose measurements were performed using a magnesium–argon ionization chamber calibrated traceable to the National Institute of Metrology of China. A schematic of this experimental configuration is provided in Fig. 2(b). The chamber was positioned at nine depths (1.6-cm intervals) within the phantom using a dedicated adjustable holder. A 5-min irradiation was performed at each position. Stable electrometer readings obtained after measurement were converted to photon dose rates using the calibration coefficients.

3. Results and discussions

3.1. Effects of D_2O substitution on tumor dose

Fig. 3 exhibits tumor dose–volume histograms (DVHs) across a range of tumor depths under varying D_2O concentrations, while Table 2 presents the corresponding tumor dosimetric parameters derived from the DVHs. The key dosimetric parameters for tumor include the maximum dose, minimum dose, mean dose, D_{80}, and homogeneity index (HI).

Firstly, the DVHs show the overall trend of the effect of D_2O substitution on dose: for tumors at four different depths, D_2O substitution leads to a steeper DVH curve, indicating that it improves dose uniformity within the tumor to some extent. Tumors at a depth of 5 cm showed reduced dose following D_2O substitution, with the dose at 20% D_2O concentration being higher than at 10%. As tumor depth increases, D_2O substitution progressively demonstrates advantages in tumor dose distribution. For tumors at 7 cm depth, the dose with 20% D_2O is higher than without substitution, while the dose with 10% D_2O is still lower. When the tumor depth increases to 8 cm, even 10% D_2O substitution enhances the dose in the tumor's low-dose regions. Table 2 further quantifies and corroborates the aforementioned changes. For tumors at 5 cm depth, D_2O substitution solely enhanced dose homogeneity, with both 10% and 20% concentrations resulting in an increase of approximately 7.1%. For tumors at 6 cm depth, 20% D_2O replacement increased the minimum tumor dose and D_{80} by 10.0% and 3.2%, respectively, demonstrating the onset of its dose-enhancing effect in deep tumor regions. When the tumor depth was increased to 8 cm, 20% D_2O substitution improved the measurements of all five key dosimetric parameters, resulting in the most significant increase of 20.4% observed in the minimum tumor dose.

Overall, results show that for the NeuPex neutron beam, D_2O substitution at concentrations below 20% does not enhance but actually diminishes the tumor dose for shallow tumors. The benefits for therapeutic dose delivery occur only when the tumor depth exceeds a specific

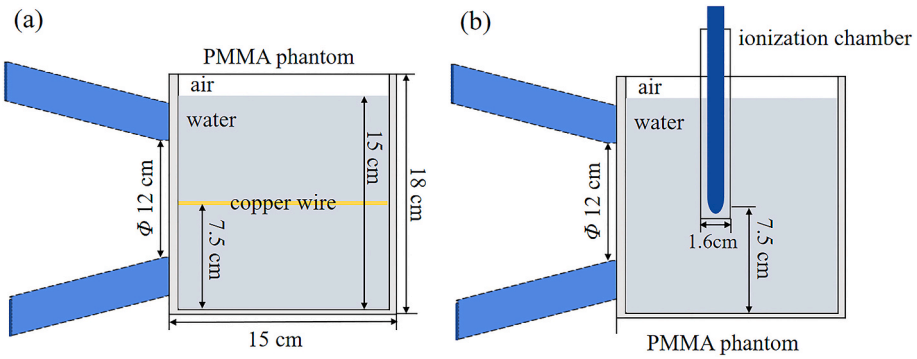

Fig. 2. Schematic of experimental configuration: (a) reaction rate measurement; (b) photon dose measurement.

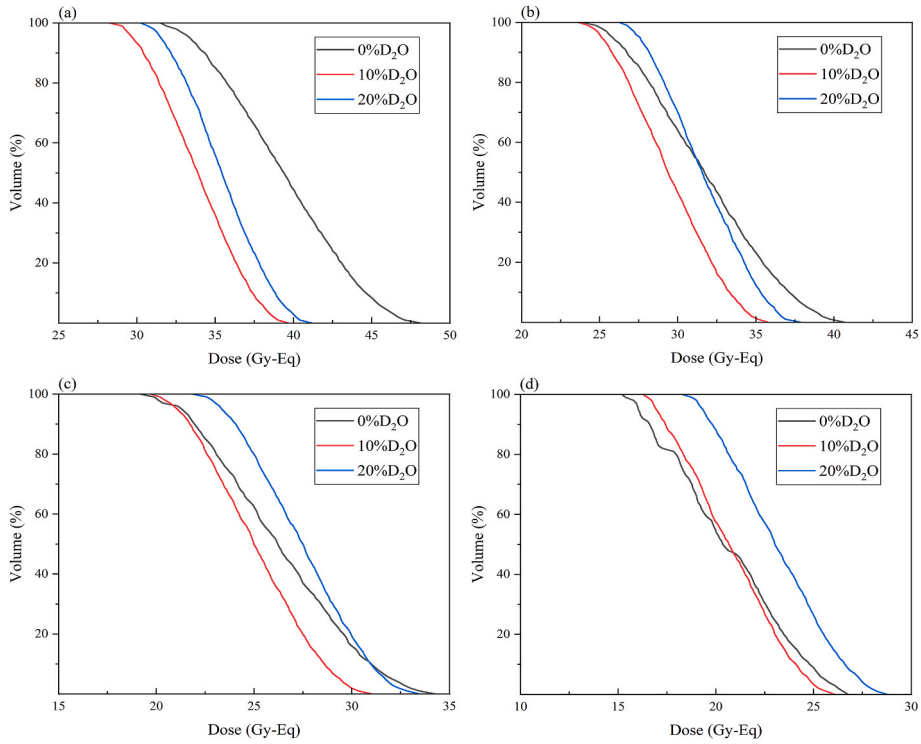

Fig. 3. Tumor dose–volume histograms (DVHs) across different tumor depths: (a) 5 cm, (b) 6 cm, (c) 7 cm, and (d) 8 cm for various D_2O concentrations.

Table 2
Key tumor dosimetric parameters across different tumor depths for various D_2O concentrations.

Depth (cm)	D_2O Concentration	D_{max} (Gy-Eq)	D_{min} (Gy-Eq)	D_{mean} (Gy-Eq)	D_{80} (Gy-Eq)	*HI*
5	0%	48.1	31.5	39.4	35.7	1.4
	10%	39.7 (−17.5%)	28.2 (−10.5%)	33.9 (−14.0%)	31.4 (−12.0%)	1.3 (−7.1%)
	20%	41.2 (−14.3%)	30.2 (−4.1%)	35.5 (−9.9%)	33.2 (−7.0%)	1.3 (−7.1%)
6	0%	40.7	23.9	31.8	28.2	1.5
	10%	35.8 (−12.0%)	23.7 (−0.8%)	29.5 (−7.2%)	26.9 (−4.6%)	1.4 (−6.7%)
	20%	37.9 (−6.9%)	26.3 (10.0%)	31.7 (−0.3%)	29.1 (3.2%)	1.3 (−13.3%)
7	0%	34.3	19.2	26.3	23.1	1.5
	10%	31.1 (−9.3%)	19.7 (2.6%)	25.1 (−4.6%)	22.6 (−2.2%)	1.4 (−6.7%)
	20%	33.5 (−2.3%)	21.9 (14.1%)	27.5 (4.6%)	25.0 (8.2%)	1.4 (−6.7%)
8	0%	26.8	15.2	20.7	18.0	1.6
	10%	26.1 (−2.6%)	16.3 (7.2%)	20.7 (0.0%)	18.3 (1.7%)	1.5 (−6.3%)
	20%	28.8 (7.5%)	18.3 (20.4%)	23.2 (12.1%)	20.7 (15.0%)	1.4 (−12.5%)

value.

3.2. *Effects of D_2O substitution on normal tissues dose*

DVHs for critical normal tissues are presented in Fig. 4 across a range of tumor depths and varying D_2O concentrations. In all cases, the treatment endpoint was the same: the maximum dose to the eyes reaching the dose limit of 5 Gy-Eq. With D_2O substitution, the volume of high-dose regions is reduced in the eyes, while an overall dose increase occurs in the skin. Conversely, brain tissue demonstrates a significant reduction in the volume of high-dose regions. Overall, D_2O substitution exerts a more limited dosimetric impact on superficial normal tissues, whereas it exhibits a comparatively larger effect on the dose delivered to deep-seated or larger-volume normal tissues.

Table 3 presents the key dosimetric parameters of critical normal tissues under varying tumor depths and D_2O concentrations. For normal tissues, key parameters comprise the maximum dose and mean dose. The impact of D_2O substitution on dose distribution differs characteristically for the eye, skin, and brain tissues. Regarding the eye, 10% D_2O substitution results in an essentially unchanged mean dose, whereas 20% D_2O leads to a slight increase. For the skin, both concentrations of D_2O produce slight increases in both the maximum and mean doses. In contrast, the maximum dose to brain tissue is significantly reduced under D_2O substitution, exceeding 16.0% across all scenarios. The mean dose to the brain also shows a reduction.

Combined with Section 3.1, these results indicate that with the NeuPex neutron beam, D_2O substitution aimed at increasing treatment depth is recommended mainly for tumor depths greater than 6 cm, and should be evaluated in conjunction with tumor size. Simultaneously, the impact of D_2O substitution differs among normal tissues, correlating with properties like tissue depth and volume.

3.3. *Effect of D_2O substitution on BNCT dose components distribution*

Previous results demonstrated dose enhancement within the tumor at a depth of 7 cm when D_2O substitution was employed. To elucidate the mechanism through which D_2O substitution influences dosimetry, deep-seated tumors at 7 cm were investigated. The depth profiles of BNCT dose components along the beam central axis were analyzed, as presented in Fig. 5.

A comparison of Fig. 5(a) and (b) reveals relatively similar distribution, particularly within the tumor region. These findings indicate not

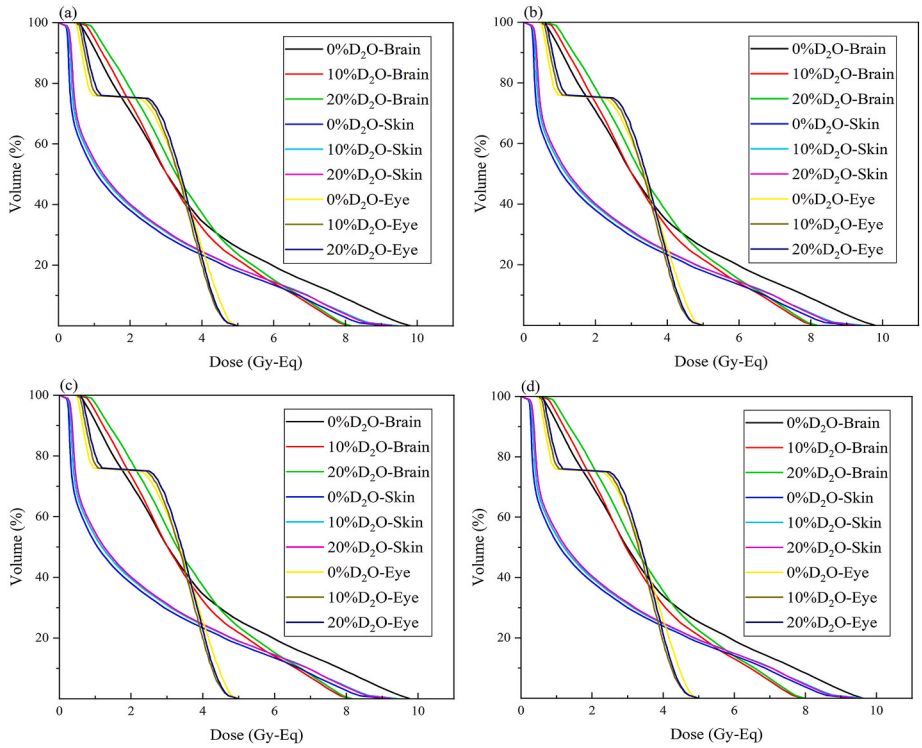

Fig. 4. Dose–volume histograms (DVHs) for critical normal tissues corresponding to tumor depths of (a) 5 cm, (b) 6 cm, (c) 7 cm, and (d) 8 cm under various D_2O concentrations.

Table 3
Key dosimetric parameters of critical normal tissues across different tumor depths for various D_2O concentrations.

Depth (cm)	D_2O Concentration	Eye		Brain		Skin	
		D_{max} (Gy-Eq)	D_{mean} (Gy-Eq)	D_{max} (Gy-Eq)	D_{mean} (Gy-Eq)	D_{max} (Gy-Eq)	D_{mean} (Gy-Eq)
5	0%	5	2.9	9.7	3.7	9.4	2.4
	10%	5	2.9 (0.0%)	7.9 (−18.6%)	3.4 (−8.1%)	9.6 (2.1%)	2.5 (4.2%)
	20%	5	3.0 (3.4%)	8.0 (−17.5%)	3.6 (−2.7%)	9.5 (1.1%)	2.5 (4.2%)
6	0%	5	2.9	9.4	3.6	9.2	2.3
	10%	5	2.9 (0.0%)	7.9 (−16.0%)	3.4 (−5.6%)	9.6 (4.3%)	2.5 (8.7%)
	20%	5	3.0 (3.4%)	8.0 (−14.9%)	3.6 (0.0%)	9.5 (3.3%)	2.5 (8.7%)
7	0%	5	2.9	9.6	3.7	9.4	2.4
	10%	5	2.9 (0.0%)	7.9 (−17.7%)	3.4 (−8.1%)	9.6 (2.1%)	2.5 (4.2%)
	20%	5	3.0 (3.4%)	8.0 (−16.7%)	3.6 (−2.7%)	9.5 (1.1%)	2.5 (4.2%)
8	0%	5	2.9	9.6	3.7	9.4	2.4
	10%	5	2.9 (0.0%)	7.9 (−17.7%)	3.4 (−8.1%)	9.6 (2.1%)	2.5 (4.2%)
	20%	5	3.0 (3.4%)	8.0 (−16.7%)	3.6 (−2.7%)	9.5 (1.1%)	2.5 (4.2%)

only that the boron dose is the dominant contributor to the total BNCT dose, but also that the effect of D_2O substitution on dosimetry primarily stems from its impact on the boron dose. Following D_2O substitution, the boron dose decreases in superficial regions but increases beyond a certain depth. This change is most likely due to the variation in the thermal neutron flux. With 10% D_2O substitution, the boron dose decreases in the superficial tumor region while increasing in the deeper region. Conversely, 20% D_2O substitution facilitates an increase in boron dose across comparatively more of the tumor volume.

The influence of D_2O substitution on the neutron dose is relatively small but regionally dependent, as shown in Fig. 5(c). Notably, it can lead to localized dose increases in specific areas. Fig. 5(d) shows that D_2O substitution significantly reduces the photon dose. However, beyond a depth of 10 cm, the photon dose shows a slight increase under the 20% D_2O condition. This behavior can be attributed to two factors: in superficial regions, the replacement of H with D reduces the probability of the H(n,γ)D reaction, thereby decreasing photon production; in deeper regions, the increase in thermal neutron flux leads to a slight enhancement of the photon dose after deuteration.

3.4. *Experimental results of D_2O substitution in the water phantom*

The depth distribution of the copper reaction rate within the water phantom at different D_2O concentrations is shown in Fig. 6(a), and the absolute value of the corresponding relative deviations are presented in Fig. 6(c). Compared to the 0% D_2O case, the 10% substitution reduces the copper reaction rate in the upper 7.2 cm but progressively increases it beyond 8.2 cm, reaching a 20.2% enhancement at 13.5 cm depth. The 20% D_2O substitution further enhanced the reaction rate increase at deeper depth, achieving a 20.3% increase at 9.3 cm and a 52.5% increase at 13.5 cm depth. The enhancing effect of 20% D_2O also becomes pronounced only from around 6 cm depth, aligning well with CHRAP simulation conclusions. Results show that D_2O substitution reduces reaction rates in shallow regions while increasing them in deeper zones. This occurs because deuterium substitution for hydrogen slows epithermal neutron moderation and absorption. Consequently, fewer

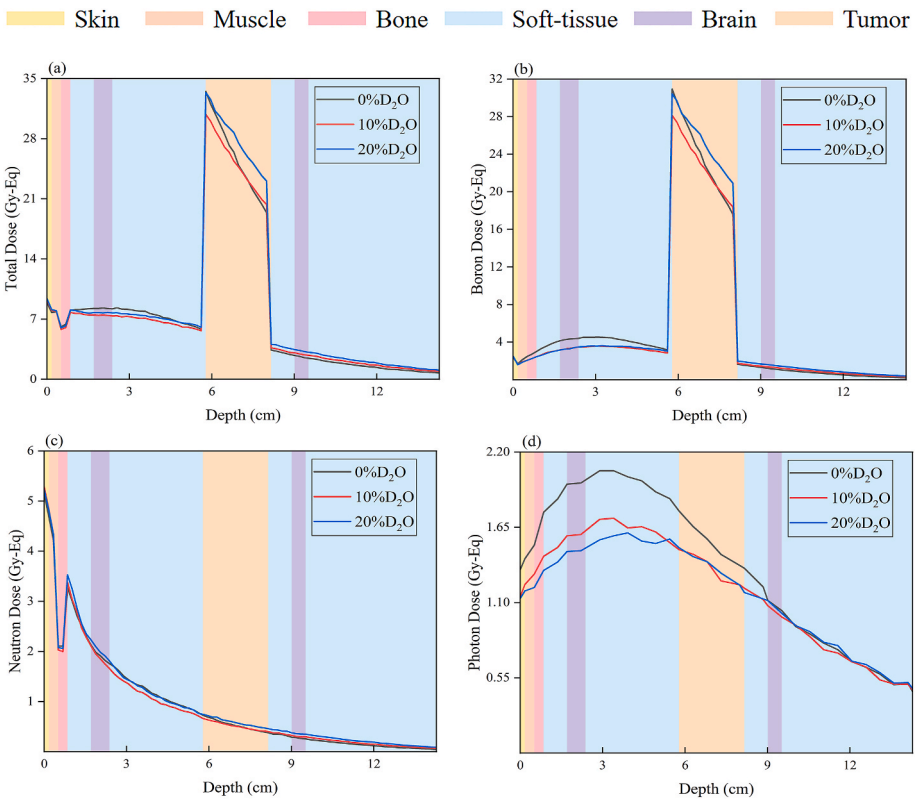

Fig. 5. Depth profiles of BNCT dose components along the beam central axis for tumor depth of 7 cm under various D_2O concentrations: (a) Total dose, (b) Boron dose, (c)Neutron dose, (d) Photon dose.

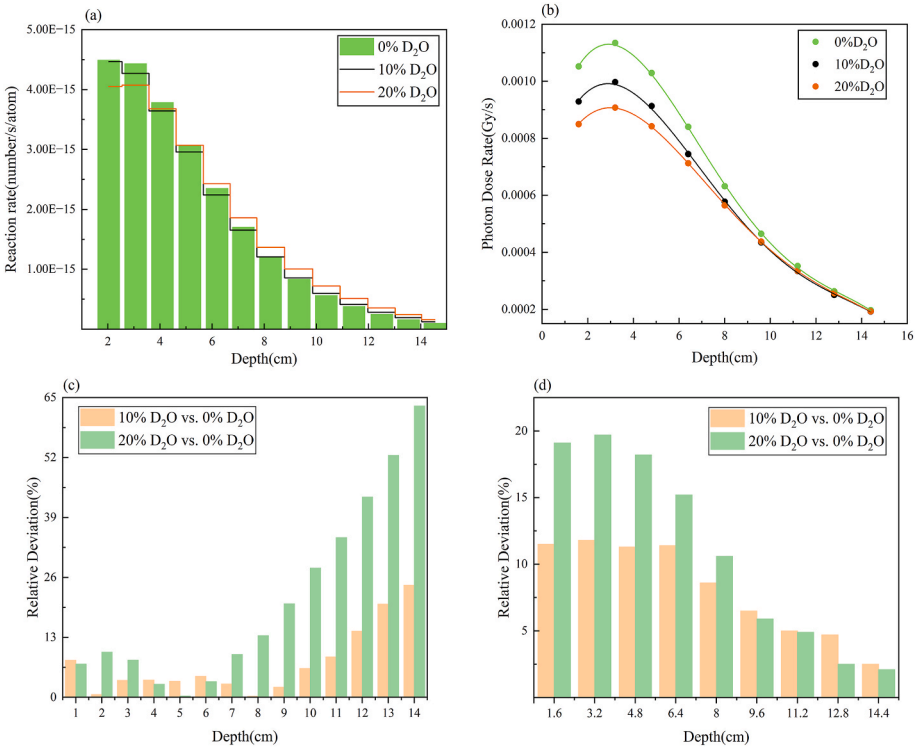

Fig. 6. Depth distributions of (a) single-nucleus reaction rate derived from $^{63}Cu(n,\gamma)^{64}Cu$ activation and (b) photon dose rate measured at varying D_2O concentrations, with (c) and (d) showing the absolute value of the corresponding relative deviations.

thermal neutrons are generated near the surface, enabling more thermal neutrons to penetrate deeper regions.

Fig. 6(b) depicts the depth distribution of the gamma dose rate within the water phantom at varying D_2O concentrations, with Fig. 6(d)

showing the absolute value of the corresponding relative deviations. At various depths, the gamma dose rate consistently decreases after D_2O substitution, with the 20% D_2O concentration exhibiting a greater reduction magnitude. The reduction in hydrogen content readily explains the diminished probability of neutron capture reactions producing 2.224 MeV gamma rays. Concurrently, the attenuation rate of the gamma-ray dose rate decreases with increasing depth, resulting from an increase in the thermal neutron flux within the deeper regions. Furthermore, D_2O substitution reduces the gamma-ray dose per unit neutron fluence, which may facilitate an increased dose delivered to the tumor while maintaining the dose to normal tissues within established clinical limits. Overall, these results demonstrate that D_2O substitution provides a feasible and effective strategy for enhancing neutron penetration while controlling photon dose in practical BNCT applications.

4. Conclusion

To address the applicability of heavy-water substitution under accelerator-based neutron sources, this study employed the NeuPex AB-BNCT system at Xiamen Humanity Hospital and a Chinese hybrid radiation phantom to systematically assess the dosimetric effects of tissue deuteration. The results indicate that D_2O substitution can significantly enhance the therapeutic dose delivered to deep-seated tumors (>6 cm). Building on this, water-phantom experiments further demonstrated that D_2O substitution increases neutron flux at greater depths while simultaneously reducing photon dose generated during irradiation. Despite these promising findings, the actual extent of tissue deuteration in vivo and its distribution across different tissues remain unclear, which may influence BNCT dose delivery and therapeutic outcomes. Therefore, animal studies are urgently needed to verify its biological effectiveness and safety, providing a basis for future clinical translation.

CRediT authorship contribution statement

Junli Ge: Conceptualization, Data curation, Writing – original draft. **Diyun Shu:** Formal analysis, Funding acquisition, Methodology, Supervision, Writing – review & editing. **Changran Geng:** Methodology, Supervision, Writing – review & editing. **Jinkai Yang:** Data curation, Writing – review & editing. **Xiaobin Tang:** Writing – review & editing. **Yuan-Hao Liu:** Writing – review & editing.

Declaration of competing interest

The authors declare that they have no known competing financial interests or personal relationships that could have appeared to influence the work reported in this paper.

Acknowledgments

This work is supported by the National Key Research and Development Program of China (Grant No.2023YFE0197700); and the National Natural Science Foundation of China (Grant No.12261131621, 12220101005).

Data availability

Data will be made available on request.

References

Barth, Rolf F., et al., 2012. Current status of boron neutron capture therapy of high grade gliomas and recurrent head and neck cancer. Radiat. Oncol. 7 (1), 146. https://doi.org/10.1186/1748-717X-7-146.

Berry, David, et al., 2015. Tracking heavy water (D_2O) incorporation for identifying and sorting active microbial cells. Proc. Natl. Acad. Sci. 112 (2), E194–E203. https://doi.org/10.1073/pnas.1420406112.

Coderre, Jeffrey A., Morris, Gerard M., 1999. The radiation biology of boron neutron capture therapy. Radiat. Res. 151 (1), 1–18. https://doi.org/10.2307/3579742. JSTOR.

Furuta, Takuya, Sato, Tatsuhiko, 2021. Medical application of particle and heavy ion transport code system PHITS. Radiol. Phys. Technol. 14 (3), 215–225. https://doi.org/10.1007/s12194-021-00628-0.

Geng, ChangRan, et al., 2014. Development of Chinese hybrid radiation adult phantoms and their application to external dosimetry. Sci. China Technol. Sci. 57 (4), 713–719. https://doi.org/10.1007/s11431-014-5480-x.

Green, S., et al., 2021. Loading Tissues with Heavy Water to Improv E Beam Penetration and Better Treat Deeper Tumours: Revisiting an Old Idea in the Modern Era of Accelerator BNCT. Book of Abstracts.

Igaki, Hiroshi, et al., 2022. Scalp angiosarcoma treated with linear accelerator-based boron neutron capture therapy: a report of two patients. Clin. Trans. Radiat. Oncol. 33, 128–133. https://doi.org/10.1016/j.ctro.2022.02.006.

Jin, Will H., et al., 2022. A review of boron neutron capture therapy: its history and current challenges. Int. J. Particle Therapy 9 (1), 71–82. https://doi.org/10.14338/IJPT-22-00002.1.

Kiger, Jingli Liu, et al., 2008. Functional and histological changes in rat lung after boron neutron capture therapy. Radiat. Res. 170 (1), 60–69. https://doi.org/10.1667/RR1266.1.

Kumada, Hiroaki, Sakae, Takeji, Sakurai, Hideyuki, 2023. Current development status of accelerator-based neutron source for boron neutron capture therapy. EPJ Techniq. Instrum. 10.1, 18. https://doi.org/10.1140/epjti/s40485-023-00105-5.

Kushner, D.J., et al., 1999. Pharmacological uses and perspectives of heavy water and deuterated compounds. Can. J. Physiol. Pharmacol. 77 (2), 79–88. https://doi.org/10.1139/y99-005.

Laissue, J.A., et al., 1983. Protection of mice from whole-body gamma radiation by deuteration of drinking water. Radiat. Res. 96 (1), 59–64. https://doi.org/10.2307/3576164.

Lee, Kyu Sun, Song, Hwa Kyung, 2021. Automation of 3D average human body shape modeling using rhino and grasshopper algorithm. Fashion Textiles 8 (1), 23. https://doi.org/10.1186/s40691-021-00249-6.

MacFarlane, Robert E., 2010. Neutron slowing down and thermalization. In: Handbook of Nuclear Engineering. Springer, Boston, MA. https://doi.org/10.1007/978-0-387-98149-9_3.

Matsumura, Akira, et al., 2023. Initiatives toward clinical boron neutron capture therapy in Japan. Cancer Biother. Rad. 38 (3), 201–207. https://doi.org/10.1089/cbr.2022.0056.

Miyatake, Shin-Ichi, et al., 2014. Boron neutron capture therapy with bevacizumab may prolong the survival of recurrent malignant glioma patients: four cases. Radiat. Oncol. 9 (6). https://doi.org/10.1186/1748-717X-9-6.

Shi, Lingyan, et al., 2018. Optical imaging of metabolic dynamics in animals. Nat. Commun. 9 (1), 2995. https://doi.org/10.1038/s41467-018-05401-3.

Takeno, Satoshi, et al., 2024. Preliminary outcomes of boron neutron capture therapy for head and neck cancers as a treatment covered by public health insurance system in Japan: real-world experiences over a 2-year period. Cancer Med. 13 (11), e7250. https://doi.org/10.1002/cam4.7250.

Valentin, J., 2002. In: Basic Anatomical and Physiological Data for Use in Radiological Protection: Reference Values ICRP Publication 89. https://doi.org/10.1016/S0146-6453(03)00002-2. United Kingdom: N , Web.

Wallace, S.A., et al., 1995a. The influence of heavy water on boron requirements for neutron capture therapy. Med. Phys. 22 (5), 585–590. https://doi.org/10.1118/1.597585.

Wallace, S.A., et al., 1995b. Monte Carlo calculations of epithermal boron neutron capture therapy with heavy water. Phys. Med. Biol. 40 (10), 1599–1608. https://doi.org/10.1088/0031-9155/40/10/003.

Wang, Ling-Wei, et al., 2018. Clinical trials for treating recurrent head and neck cancer with boron neutron capture therapy using the Tsing-Hua open pool reactor. Cancer Commun. 38 (1), 37. https://doi.org/10.1186/s40880-018-0295-y.

Zhang, Zizhu, et al., 2023. A review of planned, ongoing clinical studies and recent development of BNCT in Mainland of China. Cancers 15 (16), 4060. https://doi.org/10.3390/cancers15164060.